Supporting Information

Au nanoparticles-modified hollow carbon spheres as an advanced electrochemical sensing platform for effective detection of homocysteine in human serum

Na Li[a] , Yan Zhang[a] , Dongyu Zhang[a] , Xiaoli Zhang[a] , Ning Wei[b]*, Xiuhui Liu [a]*

[a]*Key Laboratory of Bioelectrochemistry & Environmental Analysis of Gansu Province, College of Chemistry & Chemical Engineering, Northwest Normal University, Lanzhou, 730070, China*

[b]*The first hospital of Lanzhou university, Lanzhou, 730000, China*

Other Reagent Information

Tetraethyl orthosilicate (TEOS), Formaldehyde solution (HCHO, 37.0 - 40.0 %) and Potassium ferricyanide (K$_3$ [Fe (CN)$_6$]) were obtained from Tianjin Baishi Chemical Co., Ltd., (Tianjin, China). Resorcinol (C$_6$H$_6$O$_2$, ≥ 99.5 %), Ammonia solution (NH$_3$•H$_2$O, 25 - 28 %), caustic soda (NaOH, ≥ 96.0 %) and Sodium citrate solution (C$_6$H$_5$Na$_3$O$_7$•2H$_2$O, ≥ 99.0 %) were purchased from xi'an Chemical Reagent Co., Ltd., (Xi'an, China). Chloroauric acid (HAuCl$_4$•4H$_2$O) and concentrated sulphatic acid (H$_2$SO$_4$) were obtained from Chengdu Cologne Co., Ltd., (Chengdu, China). Glutathione (GSH), uric acid (UA), Calcium chloride (CaCl$_2$), dicalcium phosphate (KCl) and cysteine (Cys), Glutamate (Glu), Xanthine (X), Dopamine (DA) and Ascorbic Acid (AA) were gained from Aladdin (Shanghai, China).
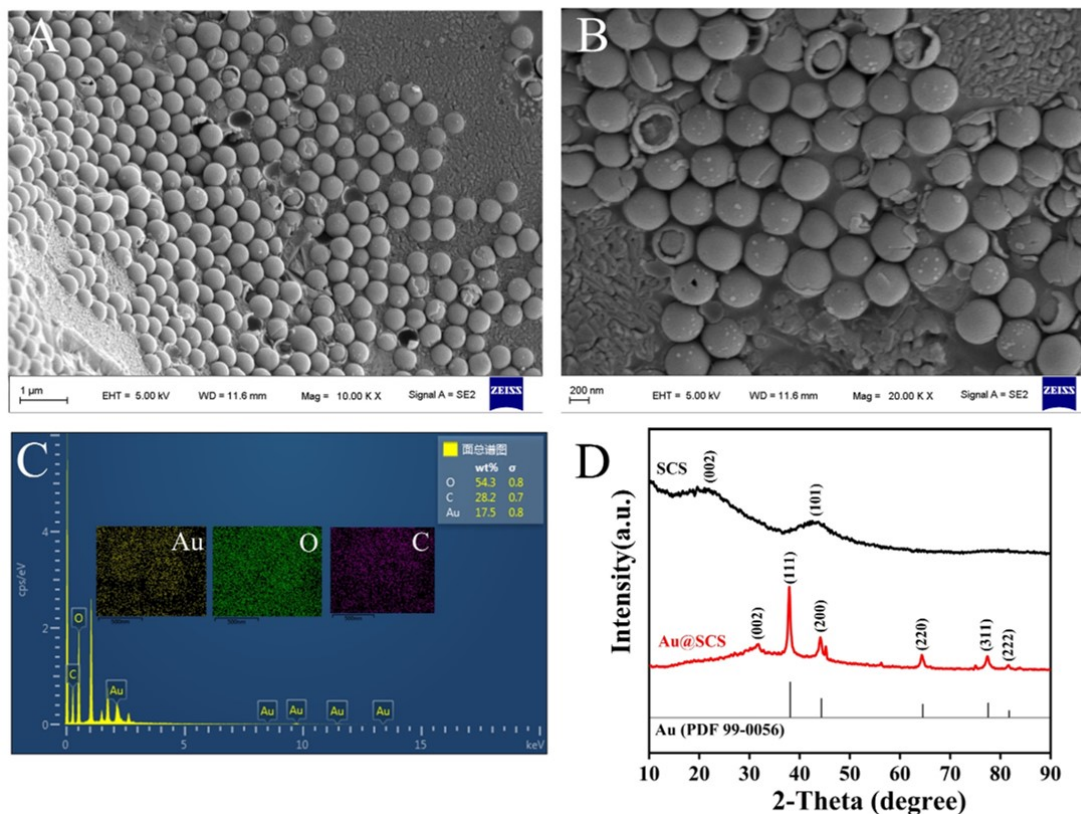
Fig. S1. (A-B) The SEM images of AuNPs@SCS. (C) The EDS mapping image of AuNPs@SCS. (D) The XRD patterns of SCS and AuNPs@SCS

Solid carbon spheres (SCSs) and AuNPs@SCSs were also prepared. In Fig. S1, the SCSs were composed of spheres with size of 400 - 450 nm. The elemental mapping of AuNPs@SCSs (Fig. S1C) confirmed the presence of three elements. Although the morphology of SCS is similar to HCS, the both structure is different. The XRD spectra (Fig. S1D) showed poor crystallinity of SCS. Because the (002) facet at 22.5° and the (101) facet at 43.5° appeared broad peaks and the intensity of the diffraction peak were weak [1, 2].
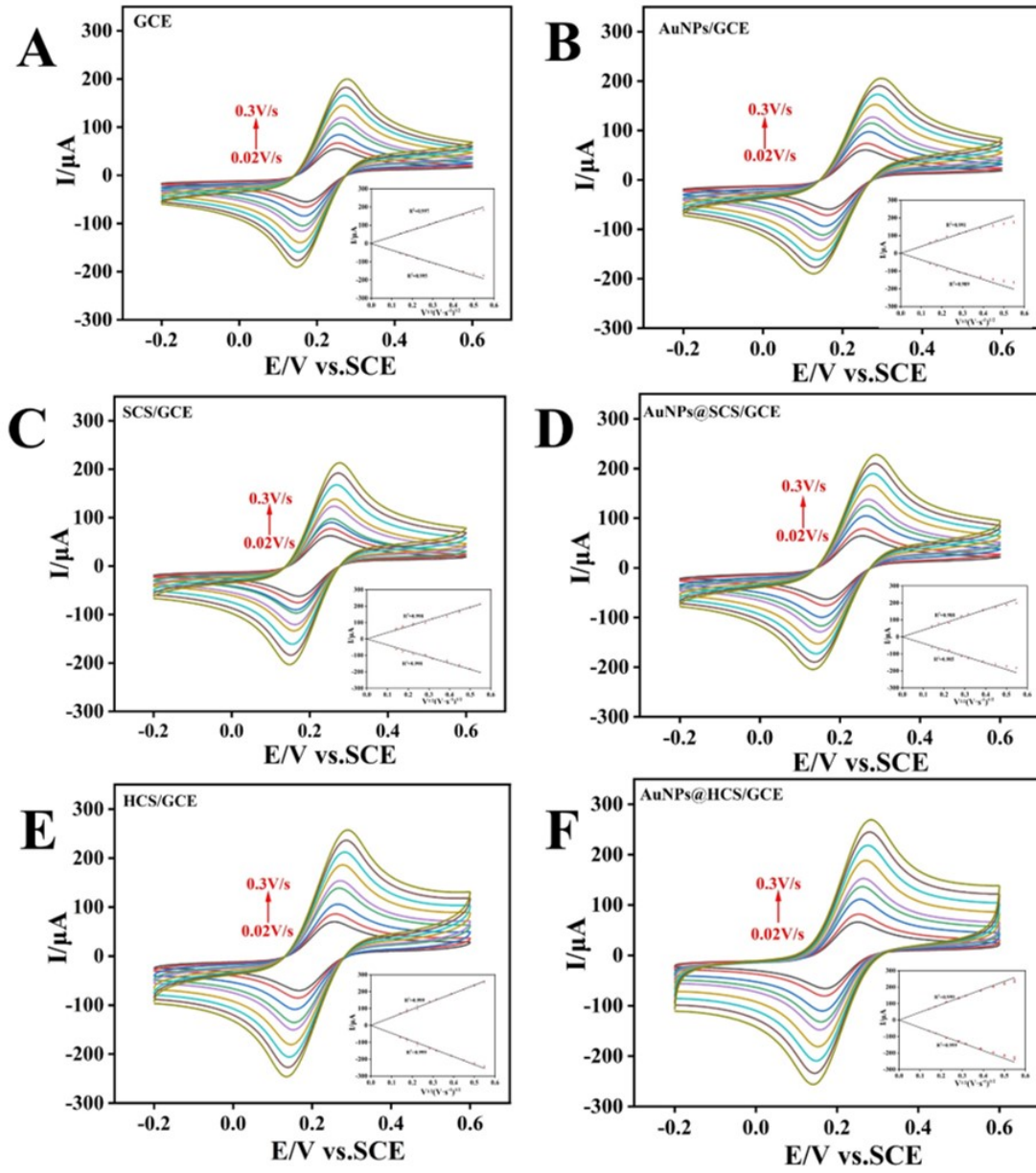
Fig. S2. CVs of different modified electrodes in 5.0 mM [Fe (CN)$_6$]$^{3-/4-}$ solution containing 0.1 M KCl with various scan rates: 0.02, 0.05, 0.08, 0.10, 0.15, 0.18, 0.20, 0.25 and 0.30 V s^{-1}. (A) bare GCE, (B) AuNPs/GCE, (C) SCS/GCE, (D) AuNPs@SCS/GCE, (E) HCS/GCE and (F) AuNPs@HCS/GCE. The insert showed plots between the square root of the scan rate (υ$^{1/2}$) and current responses (Ipa and Ipc) of different modified electrodes.

In Fig S2, we use the Randles-Sevcik formula to calculate the effective area of electroactivity for different modified electrodes[3].

$$Ip = 2.69 \times 10^5 n^{3/2} A D^{1/2} C v^{1/2} \tag{1}$$

In Eq. (1), D is the diffusion coefficient of $[Fe(CN)_6]^{3-/4-}$ ($cm^2 s^{-1}$), Ip is the peak anodic or cathodic current (μA), C is the $[Fe(CN)_6]^{3-/4-}$ concentration ($mol\ cm^{-3}$), A is the electroactive effective area (cm^2), n is the number of transferred electrons, and $\upsilon^{1/2}$ is the square root of the scan rate ($V\ s^{-1}$). The electroactive surface areas of GCE, AuNPs/GCE, SCS/GCE, AuNPs@SCS/GCE, HCS/GCE, AuNPs@HCS/GCE were calculated as 0.103, 0.110, 0.109, 0.115, 0.137 and 0.141 cm^2. The electroactive surface area of AuNPs@HCS/GCE (0.141 cm^2) was 1.37 times than that of the bare GCE (0.103 cm^2), so AuNPs@HCS/GCE is an ideal material for electrochemical sensing.
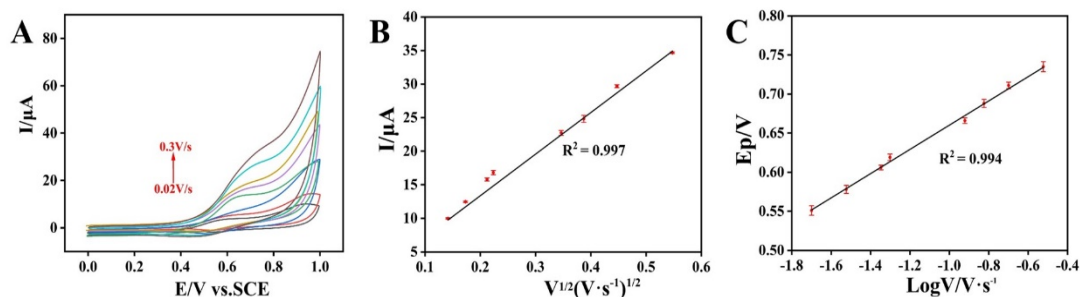
Fig. S3. (A) CVs of AuNPs@HCS/GCE in 0.2 M PBS (pH = 7.0) containing 1 mM Hcy with various scan rates 0.02, 0.05, 0.08, 0.10, 0.15, 0.20, 0.25 and 0.30 V s^{-1}. (B) The linear relationship between current responses (Ipa) and the square root of scan rates ($v^{1/2}$). (C) The linear relationship between the oxidation peak potentials (E_p) and the logarithm of scan rates (Log v).

As shown in Fig. S3A, the oxidation current (I_p) of Hcy increased with increasing scan rate. I_p of Hcy was linearly related to the square root of the scanning rate ($v^{1/2}$) in the range of 0.02 - 0.3 V s^{-1} (Fig. S3B), and the linear regression equation was Ip (μA) = 61.949 $v^{1/2}$ (V/s) + 0.975, with R^2 = 0.997. The results indicated that the electron transfer of Hcy on the surface of the modified electrode was a diffusion-controlled process[4]. In Fig. S3C, the anodic peak potential (E_p) shifted to a more positive potential with the increase of scanning rate, which indicated that the electrochemical oxidation of Hcy was irreversible. Therefore, the electrochemical oxidation of Hcy at the AuNPs@HCS/GCE in the detection of Hcy is a completely irreversible diffusion-controlled process, in which the number of electrons transferred in the electrochemical reaction can be obtained from the following equation[5].

$$\alpha n = 47.7/(E_P - E_{P/2}) \tag{2}$$

Here, E_P is oxidation peak potential, and $E_{P/2}$ stands for half-wave oxidation peak potential. For a totally irreversible electrode process, α generally is 0.500. From this, αn was calculated as 0.540. As a result, the electron transfer number (n) was further obtained to be about 1, indicating that the oxidation reaction of Hcy from Hcy (SH) to Hcy (S$^{\cdot}$) involved one electron and a proton.
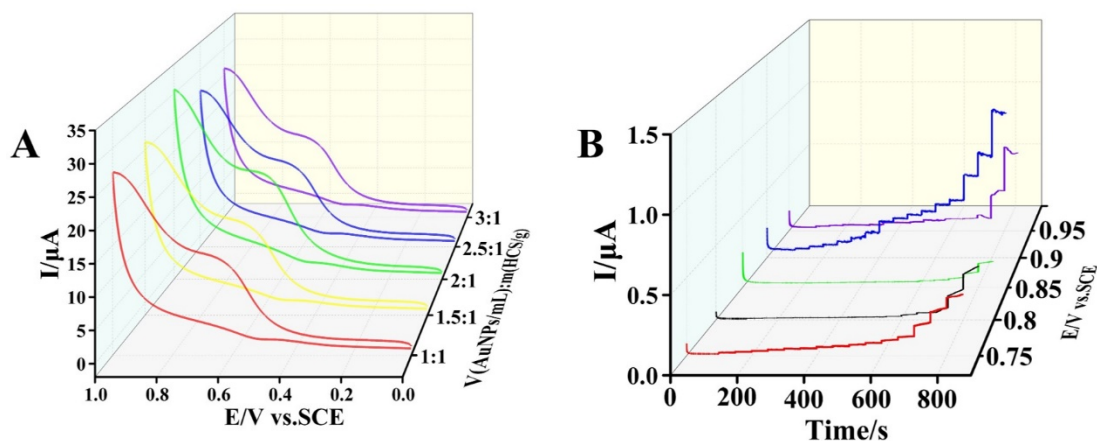
Fig. S4. (A) CV response plots of prepared AuNPs@HCS/GCE with different volume-to-mass ratios in 0.2 M PBS (pH = 7.0) contained 1 mM Hcy, at 50 mV s^{-1}. (B) Amperometric responses of AuNPs@HCS/GCE at various potentials (vs SCE) in 0.2 M PBS (pH = 7.0) with the successive addition of Hcy (13.3 nM - 21.7 μM).

In Fig. S4A, we investigated the volume-to-mass ratio of AuNPs@HCS on the electrochemical response of Hcy. The results showed that the current response of Hcy reaches the maximum value when the volume-to-mass ratio of AuNPs and HCS was 2:1; In addition, the applied potential of amperometric detection Hcy was further optimized in Fig. S4B. At + 0.90 V, the sensor exhibited the best current response.
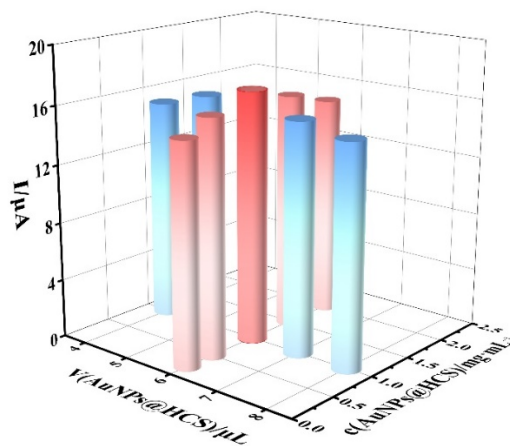
Fig. S5. Effects of deposition volume and the concentration of AuNPs@HCS/GCE, the CV responses obtained from AuNPs@HCS/GCE in 0.2 M PBS (pH = 7.0) contained 1 mM Hcy, at 50 mV s^{-1}.

In Fig. S5, we studied the effects of the deposition volume and the concentration of AuNPs@HCS on the electrochemical response of Hcy. As shown in the results, the current response of Hcy reached the maximum when the deposition volume and concentration of AuNPs@HCS were 6.0 μL and 1.0 mg mL^{-1}, respectively.
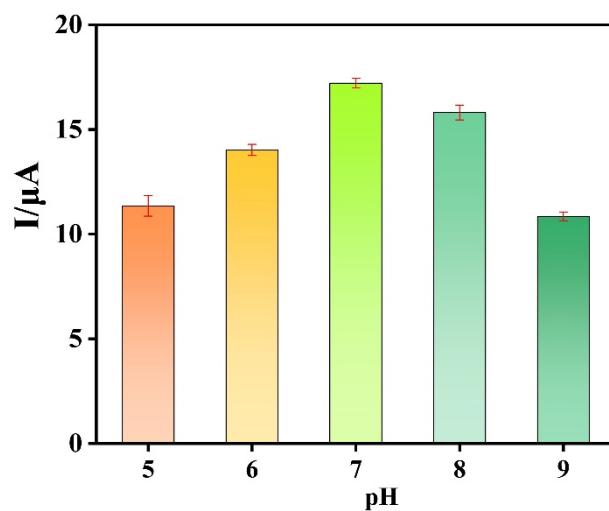
Fig. S6. Column graph of CV responses of 1 mM Hcy in different pH (range from 5 to 9) on AuNPs@HCS/GCE, at 50 mV s^{-1}.

In Fig. S6, we investigated the effect of pH of AuNPs@HCS on the electrochemical response of Hcy. The results showed that the current response of Hcy reaches the maximum value when the pH = 7.

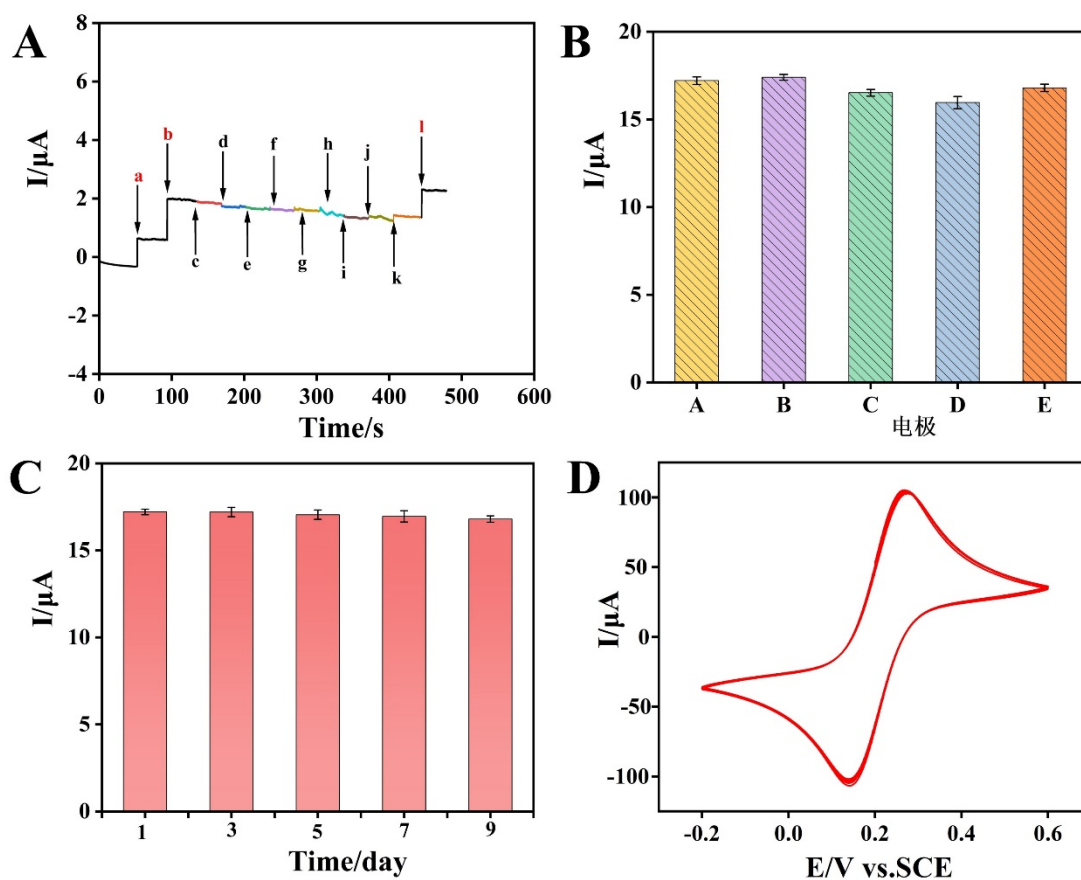The above conditions were used as the optimal experimental conditions to study the subsequent electrochemical tests.

Fig. S7. (A) Amperometric responses of the AuNPs@HCS/GCE in a 0.2 M PBS (pH = 7.0) with the successive addition of 13.3 μM of Hcy (a, b, m, and l), DA (c), AA (d), UA (e), Cl⁻ (f), Glu (g), X (h), K⁺ (i), GSH (g), Cys (k) (the concentration of the interfering substances was 66.5 μM) with potential at + 0.9 V vs. SCE. (B) Column graph of CV responses of recorded Hcy at AuNPs@HCS/GCE: 1 to 5 column graphs of CV signals of Hcy (1 mM) at five different electrodes prepared under the same conditions. (C) The stability measurements of AuNPs@HCS/GCE to 1mM Hcy for 9 days. (D) 50 segments continuous CV scanning of AuNPs@HCS/GCE in 5.0 mM [Fe (CN)$_6$]$^{3-/4-}$ solution containing 0.1 M KCl, at 50 mV s^{-1}.

Selectivity, reproducibility and stability are important indicators to determine the feasible implementation of electrochemical sensors. The selectivity of the sensor was further investigated by adding some interferences and Hcy as shown in Fig. S7A. Although the concentrations of added interferences (DA, AA, UA, Cl⁻, Glu, X, K⁺, GSH and Cys) were five times higher than those of Hcy, no marked increase in current

response occurred. The above results confirmed that AuNPs@HCS/GCE exhibited good selectivity for Hcy. Likewise, we prepared five AuNPs@HCS-modified electrodes under identical conditions to study the reproducibility of the sensor in Fig. S7B. The relative standard deviation (RSD) of the five electrode currents was equal to 1.78 %. Apart from that, the stability of the as-prepared AuNPs@HCS/GCE was evaluated via detecting the current response of 1 mM Hcy at room temperature for 9 days (Fig. S7C). After 9 days of storage, the current response remained 97.0 % of the initial current. Finally, when AuNPs@HCS/GCE was scanned for 50 segments in 5.0 mM [Fe (CN) $_6$]$^{3-/4-}$ solution containing 0.1 M KCl (Fig. S7D), the current response remained at 93.6 % of the initial current. All in all, the sensor can be used to analyze Hcy in real samples.

Reference

1.   Z. Ran, H. Yang, Z. Li, K. Wang, J. Zhao, X. Ran, G. Du and L. Yang, *ACS Sustainable Chemistry & Engineering*, 2020, **8**, 10161-10172.
2.   K. M. Kamal, R. Narayan, N. Chandran, S. Popović, M. A. Nazrulla, J. Kovač, N. Vrtovec, M. Bele, N. Hodnik, M. M. Kržmanc and B. Likozar, *Applied Catalysis B: Environment and Energy*, 2022, **307**, 121181.
3.   D. M. R. de Rooij, *Anti-Corrosion Methods and Materials*, 2003, **50**.
4.   H. Ju, X. Zhang, L. Wang, and J. Wu, *NanoBiosensing : principles, development and application*, 2012.
5.   L. R. Bard, A J, *Electrochemical Methods: Fundamentals and Applications*. 2000.